

Technical Summary of the Significant Work Accomplished

Introduction and Aim

The goal of this work is to produce creep resistance reinforcement fibers to improve the toughness and reliability of oxide ceramic composites, which are able to withstand operating temperatures of 1600°C in air. Specifically the aim was to conduct a systematic investigation of the conditions necessary for the controlled crystallization of continuous, textured or single crystal, mullite and YAG ($\text{Y}_3\text{Al}_5\text{O}_{12}$) fibers, from solid amorphous or polycrystalline fibers. This work grew out of a previous AFOSR sponsored, SBIR and STTR study in collaboration with Containerless Research Inc., Evanston, IL. In that study amorphous fibers and beads of mullite ($3\text{Al}_2\text{O}_3 \cdot 2\text{SiO}_2$) and YAG, yttrium aluminum garnet ($\text{Y}_3\text{Al}_5\text{O}_{12}$) were drawn from an aero-acoustically levitated, spinning molten bead. The quench rate was rapid, of the order of 10^3 °C/sec, and resulted in amorphous fibers of diameter 20 – 60 μm in diameter, having room temperature tensile strengths of the order of 5-6 GPa. Currently, single crystal fibers can be grown (e.g. by Saphicon Inc.) by an edge-defined method, having diameters of ~ 70 μm . However, these are expensive ($\sim \$30,000$ per kilo) and take 3 months to produce. Therefore, a more cost-effective method needs to be developed to produce creep-resistant, single crystal fibers by the mile.

Basic Science of Crystallization

The first task for this research was to see to be the determination of kinetic parameters for crystallization for amorphous YAG and mullite. To this end, spherical beads of essentially amorphous mullite and YAG were heat-treated in a sensitive DTA and DSC equipment, and then studied by X-ray diffraction and TEM. The activation energies (E_a) and enthalpies of crystallization as well as crystallization temperatures and rates were measured for both YAG and mullite as a function of temperature. Effectively "T-T-T" conditions were experimentally determined, enabling the prediction of crystallization conditions [see Johnson and Kriven, 2001]. The crystallization pathway for YAG was compared to others reported in the literature, and the occurrence of polyamorphism (polymorphs in the amorphous phase) was confirmed. Activation energy of 437 KJ/mol was measured for YAG, and crystallization could be achieved at temperatures as low as 840°C.

In the case of mullite, [Johnson, Kriven and Schneider, 2001], crystallization studies were carried out between 900 and 1400°C, using non-isothermal DSC, TEM EDS, powder XRD using standard, as well as high intensity synchrotron sources, whereby the data was analyzed by the Rietveld technique. Crystallization of the metastable, quenched spheres was observed to occur in two steps, having activation energies of 892 KJ/mole and 1333 KJ/mol, respectively. From the amorphous state, the first phases to crystallize were alumina-rich, pseudo-tetragonal mullite (~ 70 mol % Al_2O_3). These crystals were relatively large, highly strained, and contained numerous nanometer scale inclusions. With increasing temperature, the crystals were observed to incorporate increasing amounts of SiO_2 , and approach the equilibrium orthorhombic structure. By 1400°C, the pseudo tetragonal to orthorhombic transition was complete, the strain was eliminated and most of the inclusions were assimilated. There was an $\sim 67\%$ reduction in grain size and the crystals had attained the composition of the initial bulk glass (~ 60 mol % Al_2O_3). An analogy was drawn between the mechanism of crystallization of metastable mullite with recrystallization phenomena in metals, such as brass.

These studies of crystallization mechanisms in mullite are significant because they are comprehensive direct observations using state-of-the-art techniques and direct observations. They clarified a large body of theoretical and thermodynamic based literature, as well as sol gel studies, notably by Okada and co-workers, which predicted that mullite grew out of a silica matrix (Fig. 1). Our direct TEM observations indicated that exactly the opposite was true, and that silica or silica-rich inclusions grew out of large mullite grains. These subsequently crystallized to form smaller grains and relieve accumulated strains. This work pointed out the similarities in behavior of ceramics at high temperatures, with metals.

A further logical extrapolation from the work on mullite lead to the postulation of a metastable or stable syntectic invariant reaction in the alumina-silica system (Kriven 2002). A syntectic is a relatively rare, peritectic-like invariant reaction. The use of state of the art tools made this deduction possible, and this proposed phenomenon was consistent with theoretical predications as well as observations of phase separation in laser heated floated zone syntheses of melt-grown fibers.

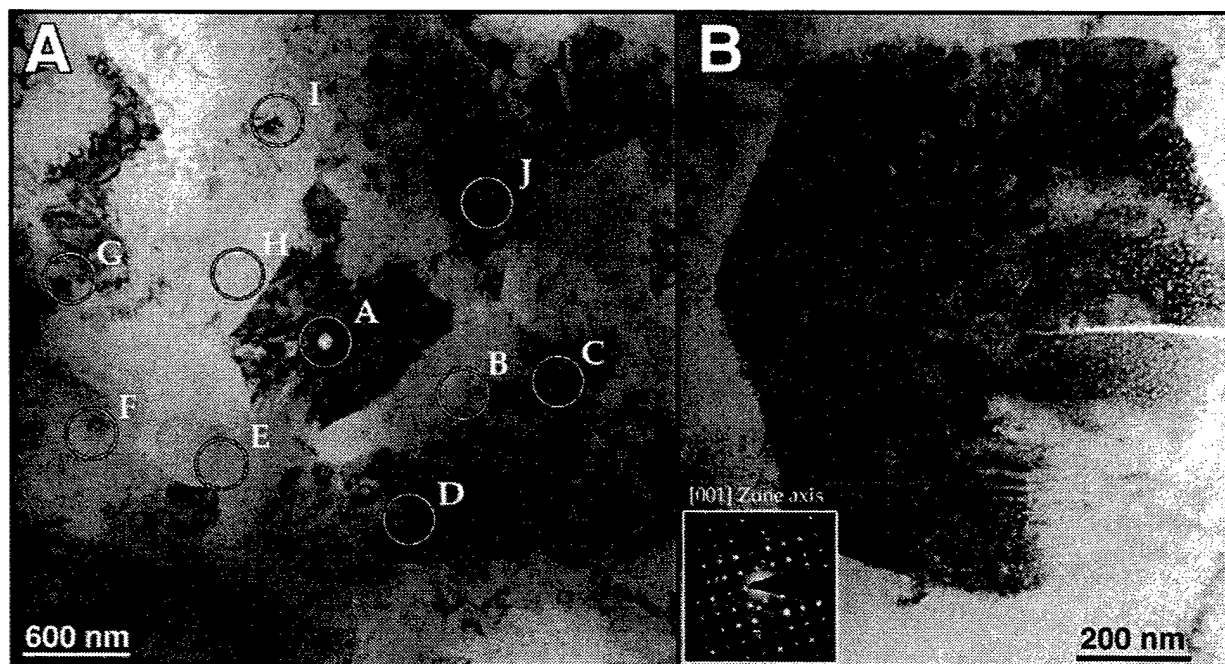


Figure 7. TEM BF images (A and B) from a polished thin section of a quenched mullite composition bead that was heated to 1085°C (M1.5). EDS analyses were made at the points labeled alphabetically, and the composition at each point was 60 ± 1 mol% Al_2O_3 , 40 ± 1 mol% SiO_2 . The variegated contrast in the grains was due to internal strain. Higher magnification of one of the grains (B) revealed small inclusions with an average size of 9.4×7.9 nm. The SAD pattern in (B) was from the [001] zone axis of a similar grain.

Fig. 1. TEM micrograph of quenched mullite as indicated in figure caption, showing silica precipitations from a large grained mullite and not vice versa as was previously commonly thought.

Experiments on Fiber Crystallization

The larger goal was to apply the basic science information towards synthesizing textured or single crystal fibers from amorphous precursors. A special machine was therefore designed and built for this purpose. It was referred to as the "fiber crystallizer" or "quadrupole furnace."

Several design criteria were identified in order to control the crystallization of amorphous fibers. Thermal energy was needed to facilitate atomic re-arrangements for crystallization. Since it would be necessary to crystallize long lengths of small diameter fibers (15 μ m), a furnace with a small hot zone could be used, so that there could be relative motion between the fiber and the hot zone. Control of atomic re-arrangement during crystallization was needed in order to create textured or single crystal fibers, so the application of a tensile force during crystallization was initially chosen as an ordering parameter. Thus, it was desired to simultaneously control fiber temperature, fiber tension, and relative motion between the fiber and the heat source. A modified floating hot zone furnace was built to accomplish these design criteria.

Electro-mechanical system

The basis for the Fiber Crystallizer was the Micropull Tensile Testing Machine apparatus purchased from Micropull Science (Thousand Oaks, CA). This machine had a computer controlled stepper motor, load cell, and LVDT used for tensile and creep testing of fibers. A Microsoft Software Disk Operating System (MS-DOS) based computer program written in Microsoft Quick BASIC 4.3 (Q-BASIC) was used to control the machine. The program sent motion instructions to a 1-axis stepper motor control card (Keithley TE5000 stepper motor control card, Keithley Instruments, Inc. Cleveland, OH). These instructions were in turn sent to a micro-step power drive (P351 microstep power drive, American Precision Instruments, (API Motion) Amherst, NY) which converted the distance, direction, speed instruction signal into pulses to move the stepper motor (API M231-02). The stepper motor was attached to a linear rail (LM guide actuator type KR3306A + 100LP-01600, THK Co., LTD, Tokyo, Japan), and as the motor turned, it turned a lead screw that caused a small block to move linearly along the rail. A load cell (Sensotec 10 lb load cell with Sensotec in-line amplifier, Sensotec Inc., Columbus, OH) was attached to this block, and one of the fiber testing grips was attached to the load cell. The other grip was stationary. An LVDT (Solartron DG 1.0, (Solartron Metrology, Gastonia, NC) with an Entran PS-15-1 power supply (Entran Devices Inc., Fairfield, NJ)) was positioned (adjustable) between the stepper motor and the motion block. It was used to measure displacement during testing. The data from the load cell and the LVDT was read by an analog to digital converter (ADC) card (Keithley ADC 16 analog to digital converter) in the computer, and was recorded by the program and used for feedback purposes. Since the Micropull was effective at controlling fiber tension, it was decided to build a similar linear motion rail assembly and mount a furnace on it. A furnace controller would be used to control fiber temperature, and a computer-controlled, linear rail assembly would translate the furnace along the length of the fiber axis.

In essence, the existing Micropull testing apparatus was modified to accommodate a second, stepper motor driven, linear rail assembly. The existing single axis stepper motor control card (Keithley TE5000) was traded in for a 2-axis card capable of simultaneously controlling the motion of two stepper motors. An additional micro-step power drive (API P261) was purchased along with an additional stepper motor (API M231-02) and another linear rail ((LM guide actuator type KR3306A + 600LP-01700, THK Co., LTD, Tokyo, Japan)) which was 600mm long. Both linear rail assemblies were then mounted on the same base plate. This base

was constructed so that the Fiber Crystallizer could be operated in either a horizontal or vertical configuration.

Quadrupole Furnace

A quadrupole lamp furnace was used as the heat source for the Fiber Crystallizer. This furnace consisted of four Osram Xenophot® HLX Xenon lamps (HLX 64635, 15V, 150W, OSRAM SYLVANIA, Palo Heights, IL) which consisted of a xenon filled, tungsten filament, halogen bulbs with a gold-plated, glass, elliptical reflector. The relative spectral intensity of the lamps (taken from the manufacturer's literature) is shown in Fig. 2. The lamps are constructed so that the light source is at one focal point of the elliptical reflector, and the other focal point is approx. 19 mm away from the tip of the bulb. A drawing of a cross-section of an HLX 64635 lamp is shown in Fig. 3. The lamps were arranged in a machined tetragonal housing, machined out of brass, so as to have a common focal point in order to simultaneously concentrate all of the radiation from the four lamps at one point.

The tungsten filament in the bulbs is fashioned into a coil that goes across the diameter of the bulb. This allows two types of bulb alignments. The first configuration is with all of the filaments arranged parallel to the length of the furnace, this is called the "hot rod" configuration (Fig. 4), since the hot zone is cylindrical in shape along the axis of the furnace. The other configuration is called the "hot spot" arrangement (Fig. 4) with all of the filaments aligned perpendicular to the axis of the furnace. It was given this name because the hot zone formed is more disk-shaped. The temperature profile through the furnace was measured by positioning a Pt-Rh thermocouple along the center axis of the furnace, and recording the temperature. This was done for both the bulb configurations (Fig. 5).

This type of furnace was chosen for several reasons. It was capable of extremely hot temperatures (in excess of 1835°C, T_{mp} of B-type thermocouples), it was capable of rapid heating and cooling rates ($\sim 100^\circ\text{C}/\text{min}$) due to its small thermal mass, and large temperature gradients are possible since all of the energy is focused on a small area (an elliptical region approximately 2 mm in diameter and 5 mm long in the center of the furnace).

Fig. 6 is a contour plot of fiber temperature as a function of quadrupole furnace speed and furnace temperature for the Fiber Crystallizer.

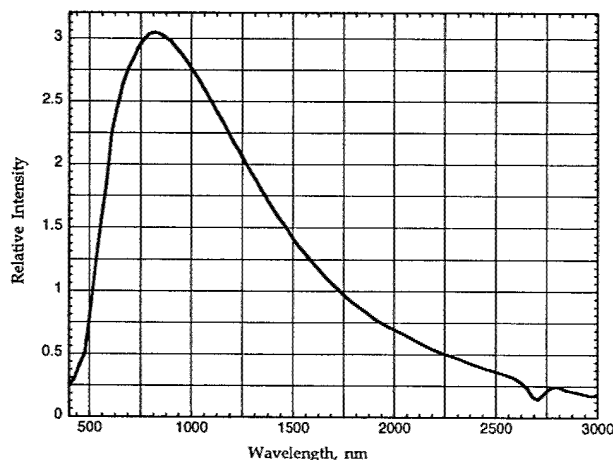
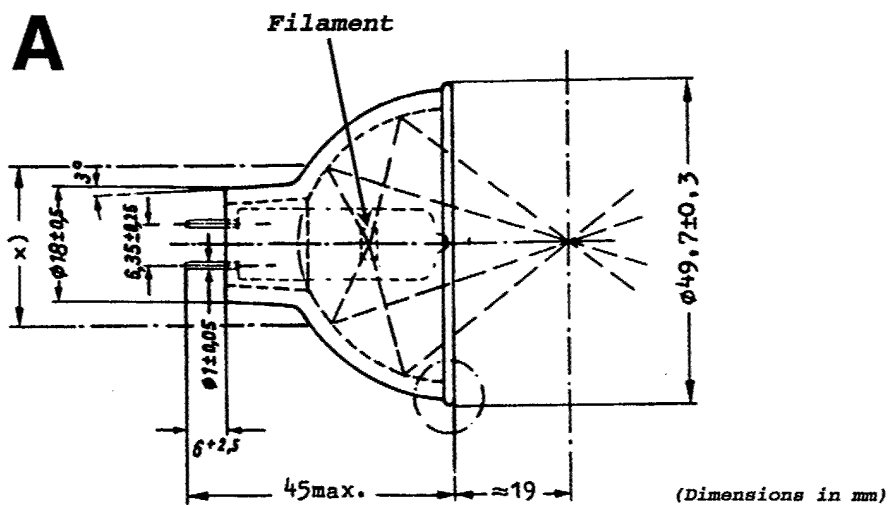
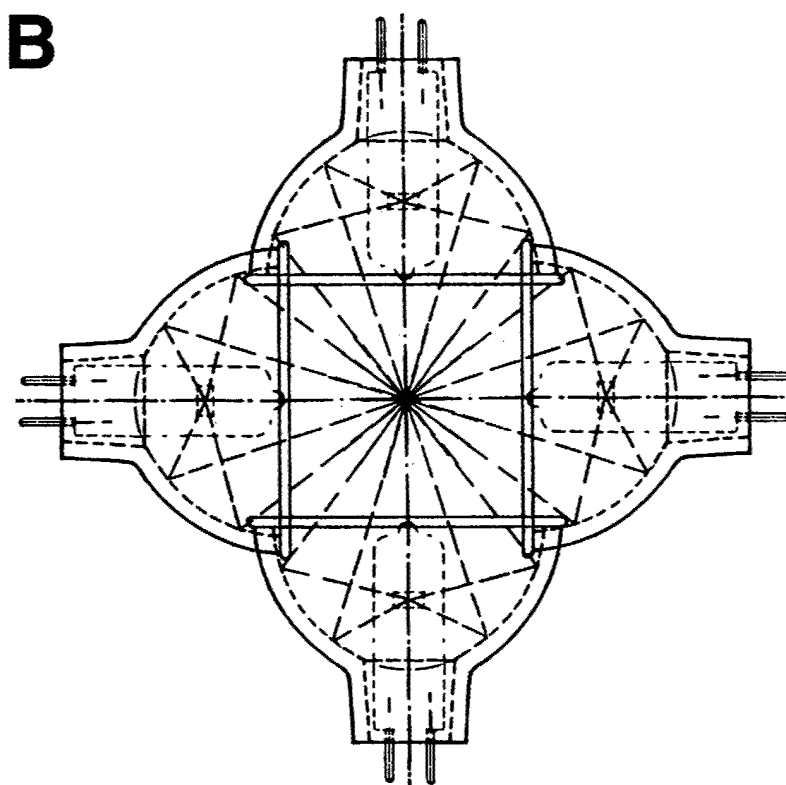


Fig. 2. Relative spectral intensity (relative intensity vs. wavelength) for OSRAM HLX 64635 Xenophot® infra-red reflector lamps (taken from the manufacturer's data).



Side view, "hot rod" configuration.



Top view, "hot spot" configuration.

Fig.3. Cross sectional views of OSRAM HLX 64635 Xenophot® lamps. The side view (with dimensions) is shown in (A), and a top view of four lamps (such as in the quadrapole furnace) is shown in (B).

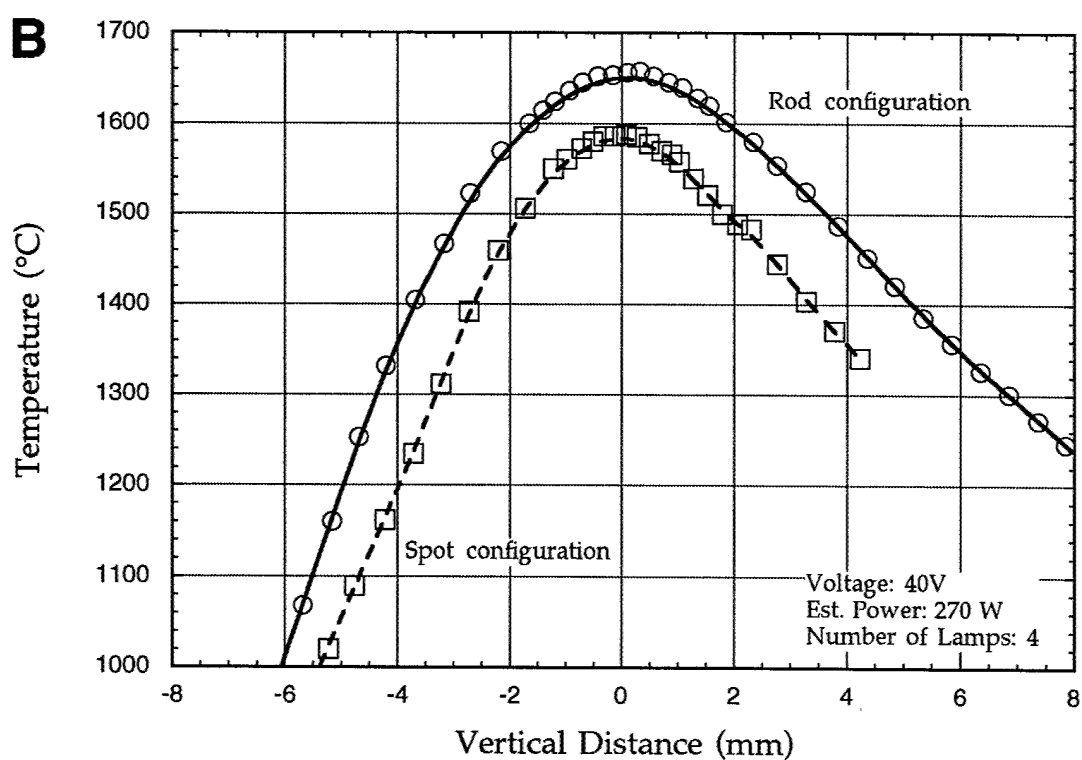
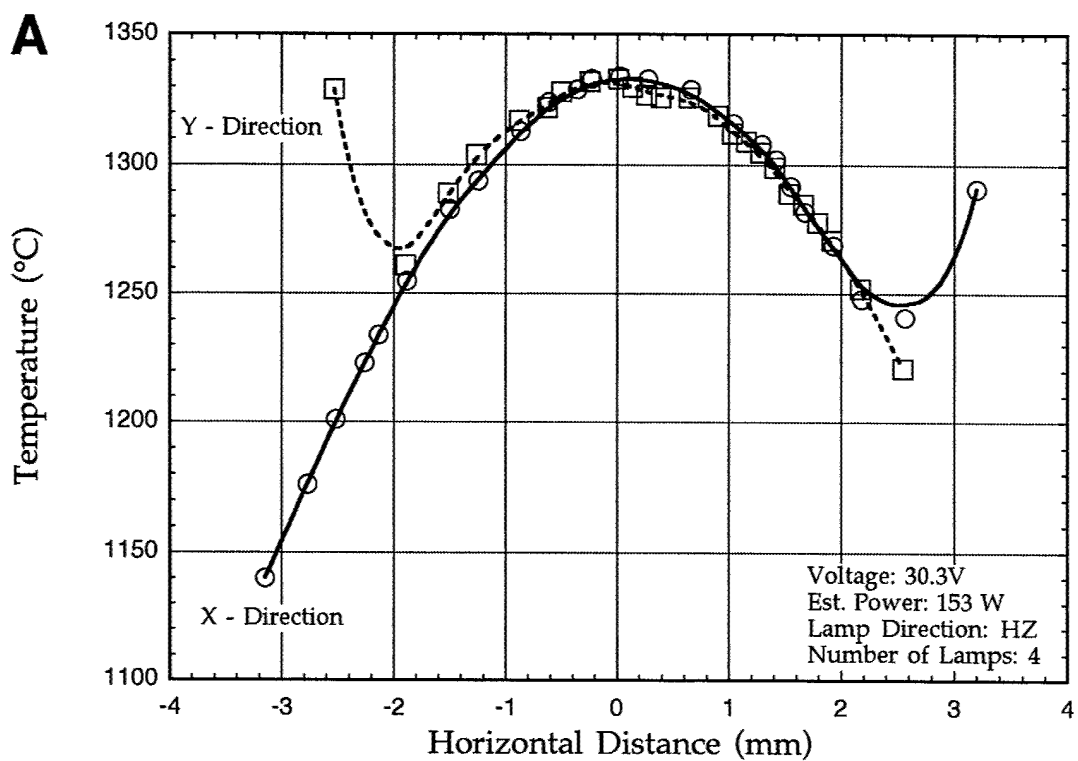


Figure 4. Temperature profile through the quadrupole lamp furnace in the “hot rod” and “hot spot” configurations. (Courtesy of Dr. Dong Zhu.)

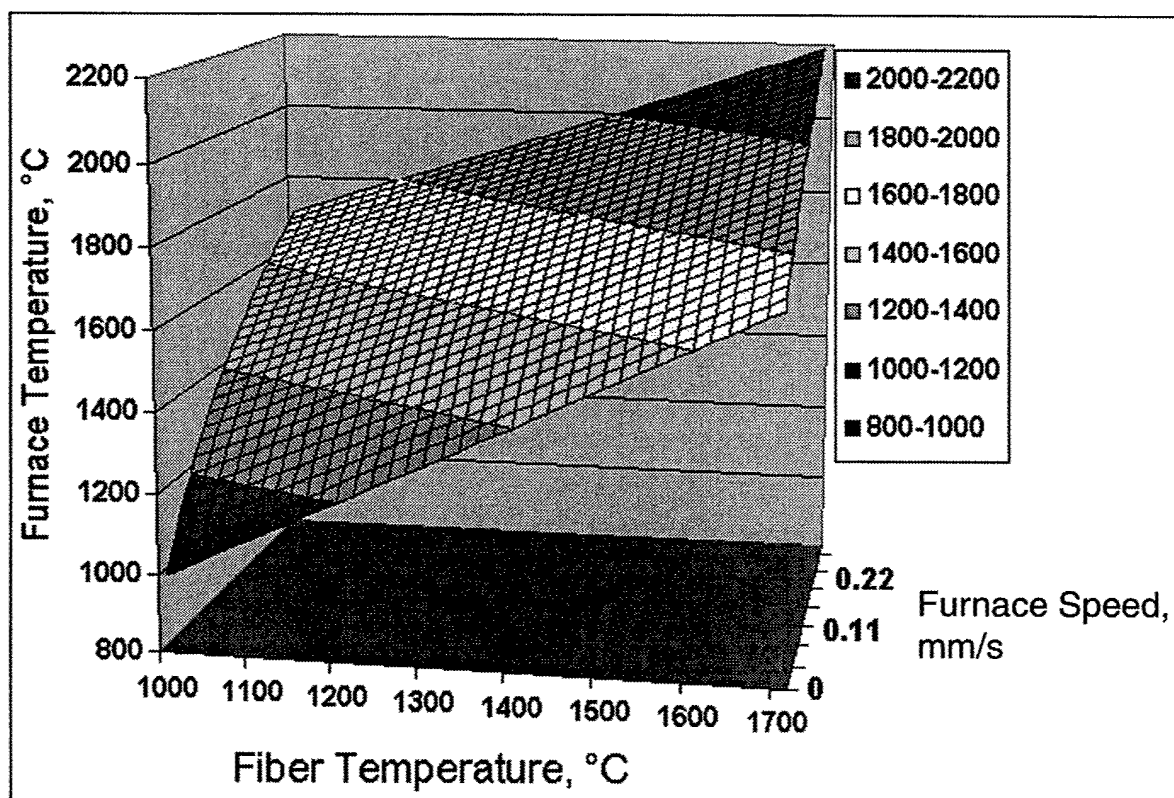


Fig. 5. Contour plot of fiber temperature as a function of quadrupole furnace speed and furnace temperature for the Fiber Crystallizer.

More recent progress has focussed on precise temperature calibration of the fiber crystallizer and studying the effects of temperature and traverse rate on the microstructure. A comprehensive summary of progress is given in the Appendix.

Conclusions

- We have studied crystallization mechanism of quenched YAG and mullite and determined the parameters of kinetics and thermodynamics. This has enabled us to put together T-T-T curves for both systems.
- We have built and calibrated a four-lamp, image furnace, having a narrow hot zone and capable of operating to 2000°C in air
- Heat treatments can be controlled by two parameters of temperature and traverse rate (from 0.1 mm/sec to 0.025 m/sec, or 1 inch/sec)
- Grain growth, densification and melting can be achieved in monofilaments, indicating the feasibility of making textured or single crystal fibers in a continuous process.
- We have developed a process to extrude polycrystalline powders of green diameters ~150 μm , which densify to ~100 μm or less
- Nextel 550, 720, pure and TiO_2 -doped mullite fibers have been heat treated or melted, and a textured microstructure has been achieved.

Personnel

Bradley R. Johnson (Ph. D. student)
Wonki Yoon (Ph. D. student)
Dr. Dong Zhu (post doctoral research associate, was partially funded briefly)

Graduate Theses

- "Kinetics and Pathways for Crystallization of Amorphous Mullite and YAG," Ph.D. thesis by Bradley R. Johnson, submitted to the University of Illinois at Urbana-Champaign, Department of Materials Science and Engineering, March (2001). Professor W. M. Kriven, thesis advisor.

Publications in refereed journals

- "Crystallization Kinetics of Yttrium Aluminum Garnet ($Y_3Al_5O_{12}$)," B. R. Johnson and W. M. Kriven, *J. Mater. Res.*, **16** [6] 1795-1805 (2001).
- "Crystal Structure Development during Devitrification of Amorphous Mullite," B. R. Johnson, W. M. Kriven and J. Schneider, *J. Europ. Ceram. Soc.*, **21** 2541-2562 (2001).
- "Crystallization Mechanism of Amorphous Mullite and the Alumina-Silica Phase Diagram," W. M. Kriven, (invited lecture) *Mat. Res. Symp.* vol. **702**, 303-309 (2002).

Publications in Conference Proceedings

- "TEM Characterization of Pseudotetragonal Mullite," B. R. Johnson and W. M. Kriven, *Proc. Microscopy and Microanalysis Society Annual Meeting*, vol **7**, Supplement 2, 426-427 (2001).

Conference Presentations (** indicates invited lectures, * indicates awards)

- * "Crystallization-Microstructure-Property Relations of Amorphous Mullite and YAG Fibers," B. R. Johnson* and W. M. Kriven." Abstract [C-067-00], presented at the 24th Annual Cocoa Beach Conf. and Expo. and Int. Conf. on Engineering Ceramics and Structures, held at Cocoa Beach, Florida, Jan 23-28th, 2000. The paper was awarded the "Third Place Best Paper Presentation Award" (in student category).
- "Crystallization-Microstructure-Property Relations of Amorphous Mullite and YAG Fibers," B. R. Johnson* and W. M. Kriven." Presented at the 102nd Annual Meeting and Exposition of the American Ceramic Society, April 30th – May 3rd, St. Louis, Missouri 2000.
- ** "Oxide Fibers and Interphase Debonding Mechanisms," W. M. Kriven,* B. R. Johnson, S. J. Lee, C. M. Huang, D. Zhu and Y. Xu. Presented at Int. Conf. On Processing of Fibers and Composites, held in May 21-26, 2000, Tuscany Italy.

- ** "Progress in Microstructural Design for Tough, Oxide Ceramic Composites," W. M. Kriven,* (invited keynote lecture) Australian International Conference on Ceramics (Austceram) 2000, held in Sydney Australia, June 25th – 28th 2000.
- ** "Crystallization Mechanisms and Microstructures in Mullite," W. M. Kriven,* and B. R. Johnson, R. A. Gronsky and J. A. Pask (invited lecture) presented at Mullite 2000 Workshop, taking place on the Isle of Mull, Aug 28th to 30th, 2000.
- ** "Design of Oxide Composites with Debonding Interphases," W. M. Kriven*. Presented at 25th Annual International Conf. on Advanced Ceramics and Composites, Jan 21-26 (2001) Cocoa Beach, Florida.
- "Crystallization Mechanism of Melt-Quenched, Solid Amorphous Mullite," B. R. Johnson, W. M. Kriven* and J. Schneider. Presented at 25th Annual International Conf. on Advanced Ceramics and Composites, Jan 21-26 (2001) Cocoa Beach, Florida.
- ** "Design of Oxide Composites with Debonding Interphases, W. M. Kriven*. Presented at Int. Conf. on Materials Science and Technology, April 2-4, (2001), Cairo, Egypt.
- "TEM Characterization of Pseudotetragonal Mullite," B. R. Johnson* and W. M. Kriven, Presented at Annual Meeting of the Microscopy and Microanalysis Society, Aug 5-9, (2001) Long Beach, CA.
- ** "Energy Dissipation by Martensitic Transformations in Ceramics," W. M. Kriven,* Pacific Rim (PAC RIM) 4 Conf., held in Maui, Hawaii, Nov 4-8 (2001).
- ** "Crystallization Mechanisms of Amorphous Mullite and the Al_2O_3 - 2SiO_2 Phase Diagram," W. M. Kriven,* presented at the Annual Meeting of the Materials Research Society, Boston, MA, Dec 2001.
- ** "Oxide Ceramics with Debonding Interphases", W. M. Kriven* (invited plenary lecture), Annual Meeting of the Korean Ceramics Society, held in Seoul, Korea, April 19th (2002).

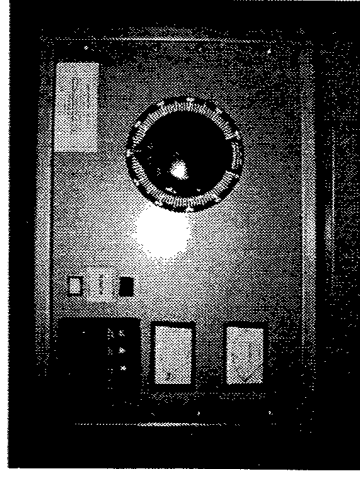
New Discoveries, Patents, Inventions

None

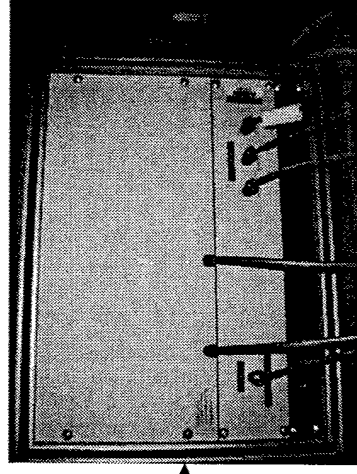
Appendix

Controlled Crystallization of Amorphous Oxide Fibers

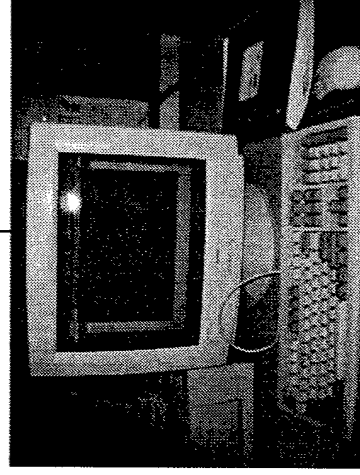
Crystallizer



Power Controller



Controlling unit



Computer control

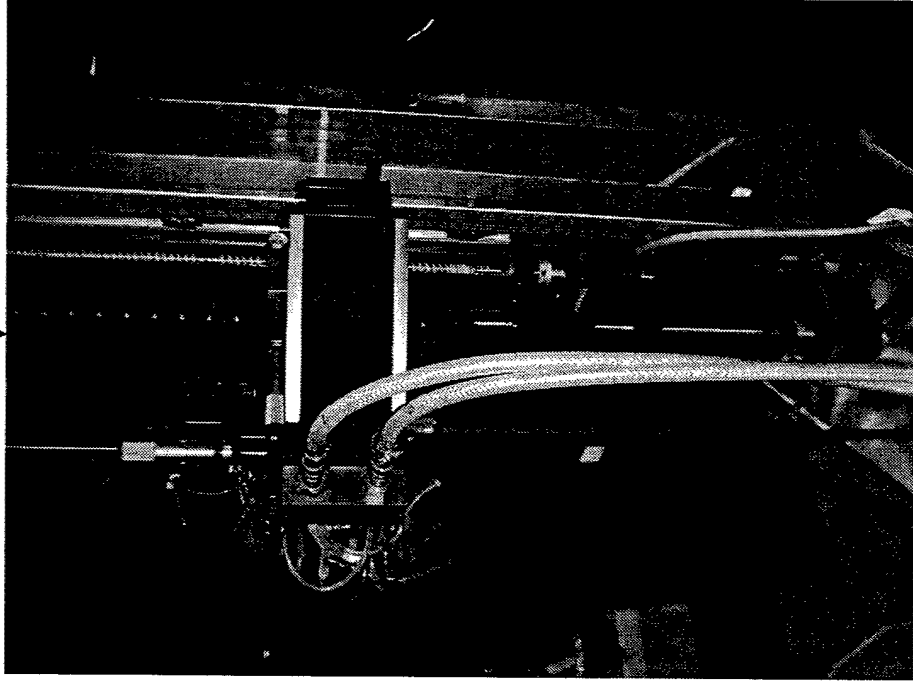


Image Crystallizer

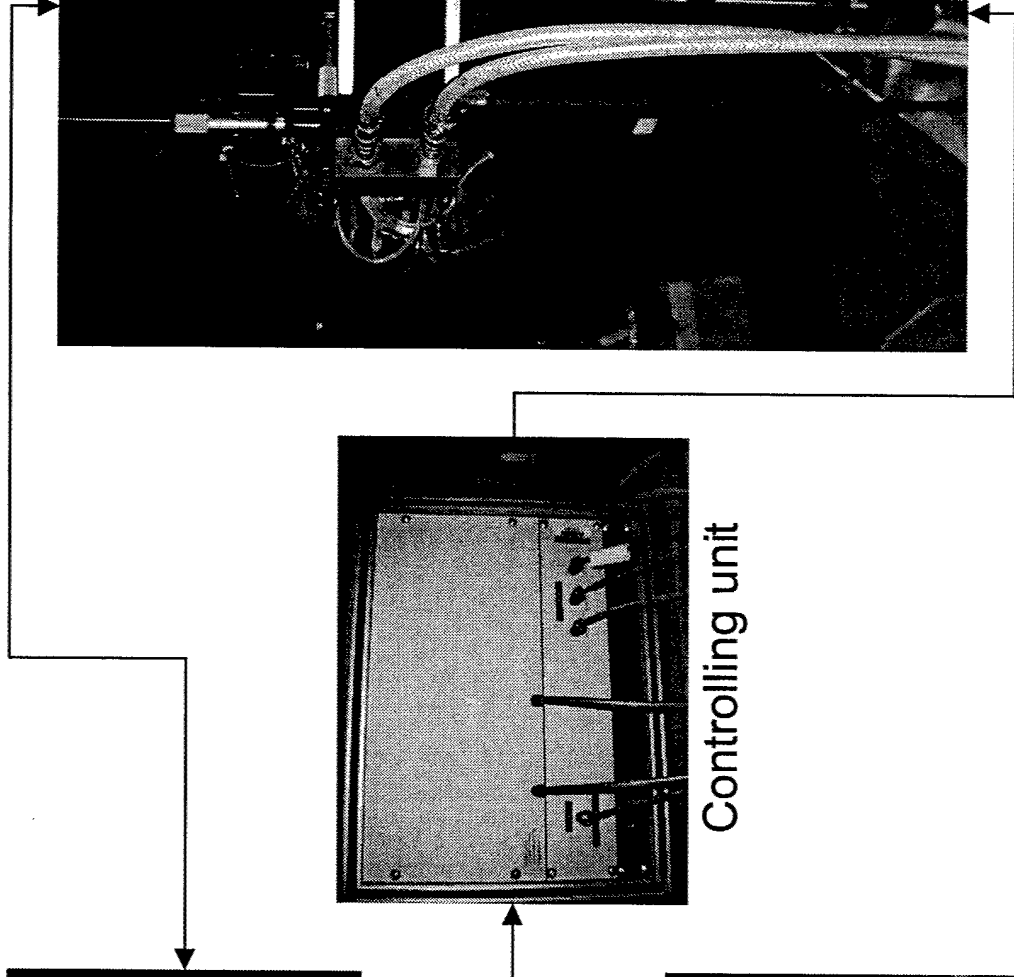
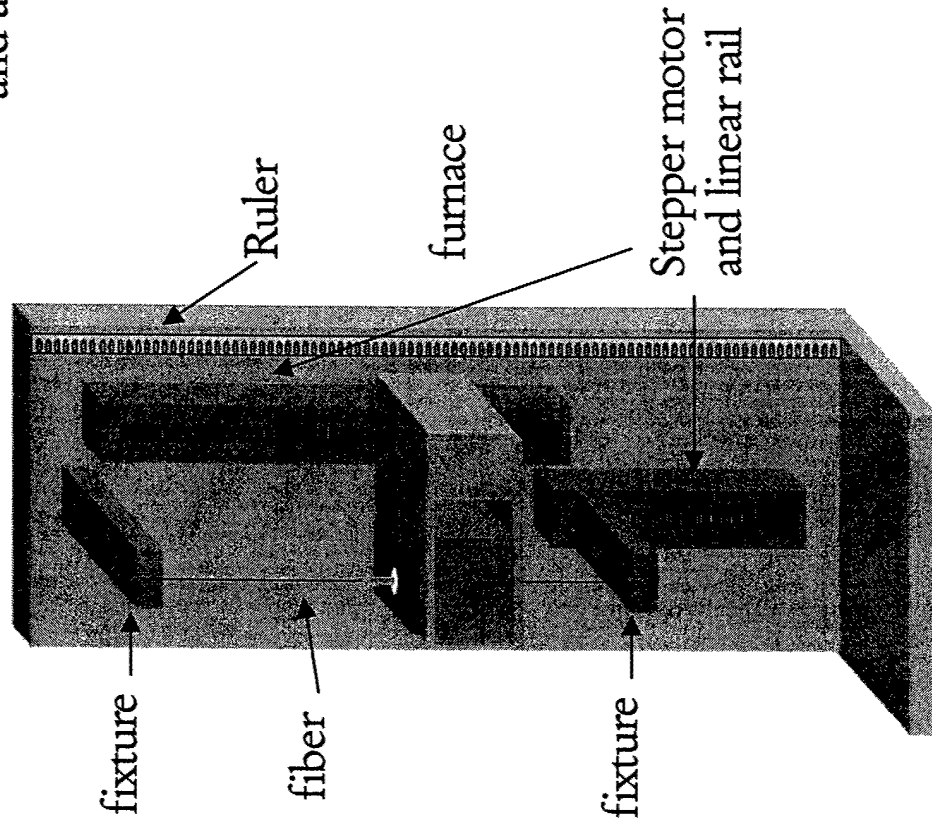
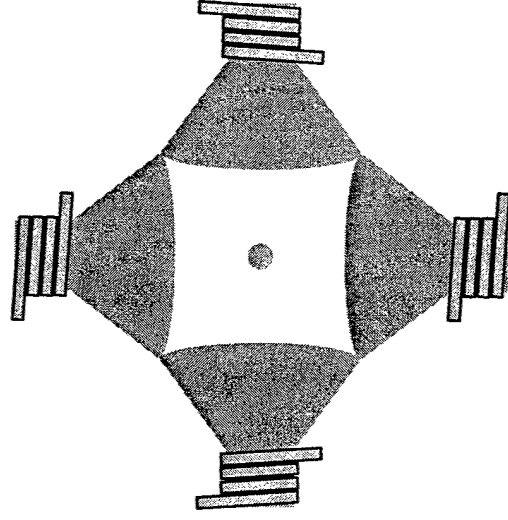
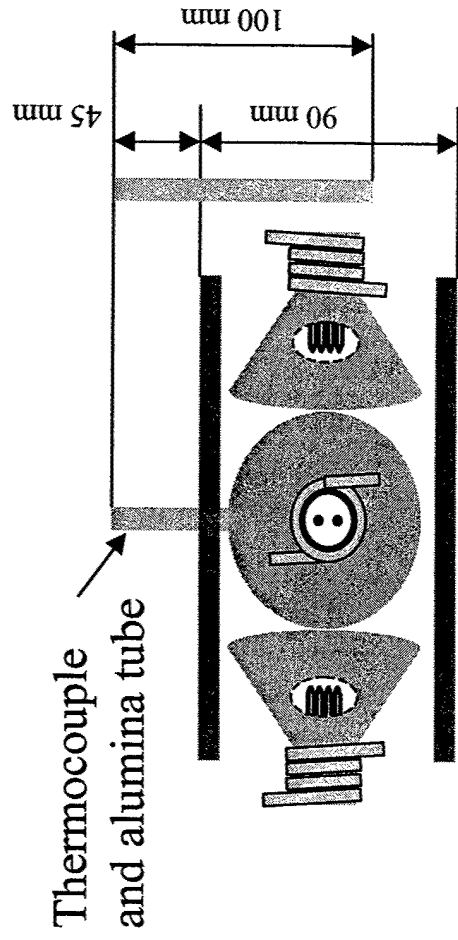
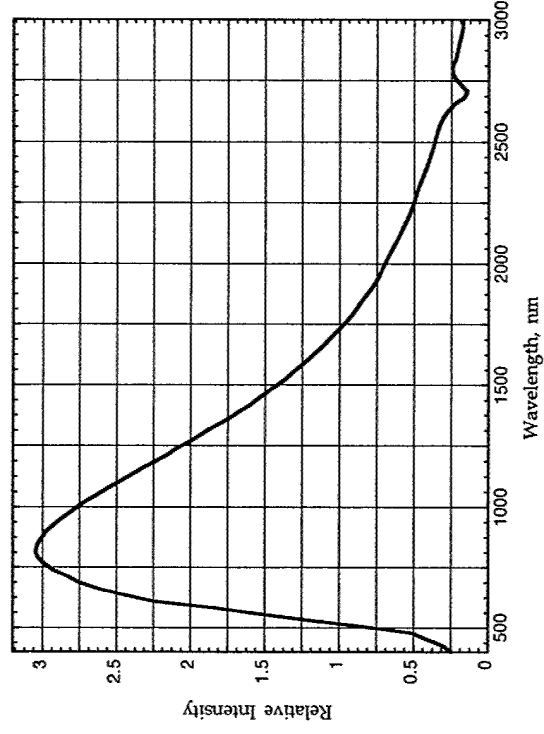
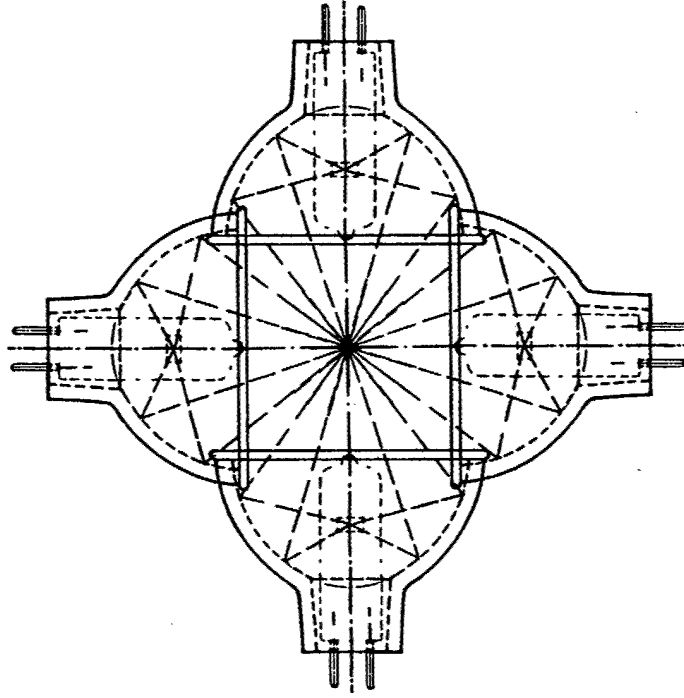


Image furnace



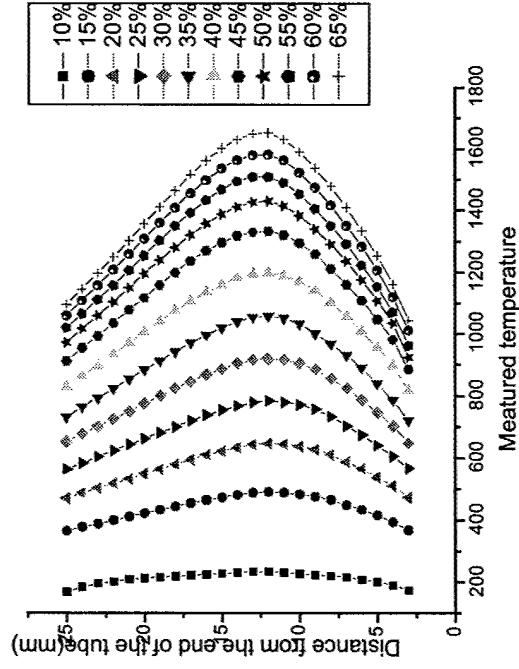
Lamp

Halogen lamps are used in hot spot position

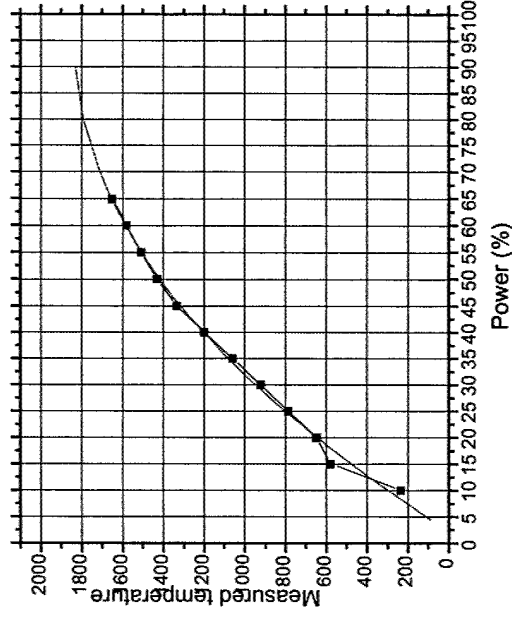


Radiation of the halogen lamp

Temperature measurement

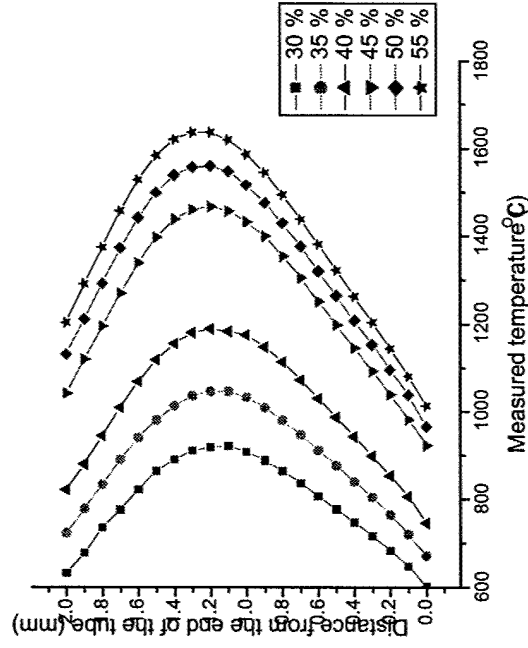


Temperature measurement
Hot rod with Al_2O_3 tube
 (OD : 6 mm, ID : 5 mm)

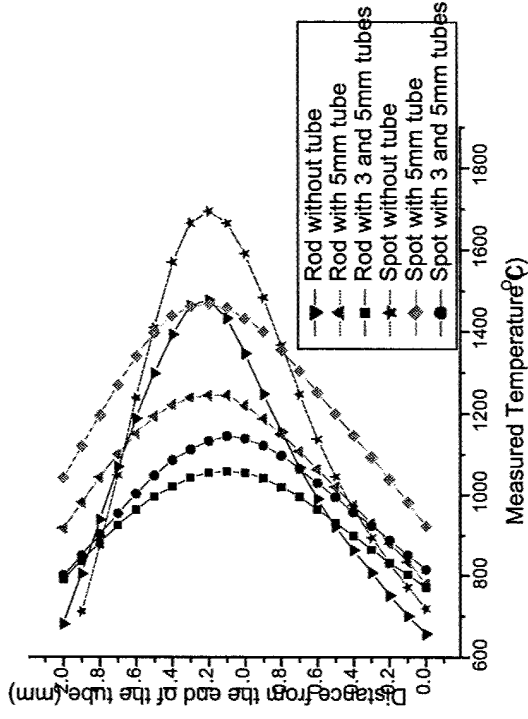


Measured vs. expected
temperatures with one Al_2O_3
tube (OD : 6 mm, ID : 5 mm)

Temperature measurement

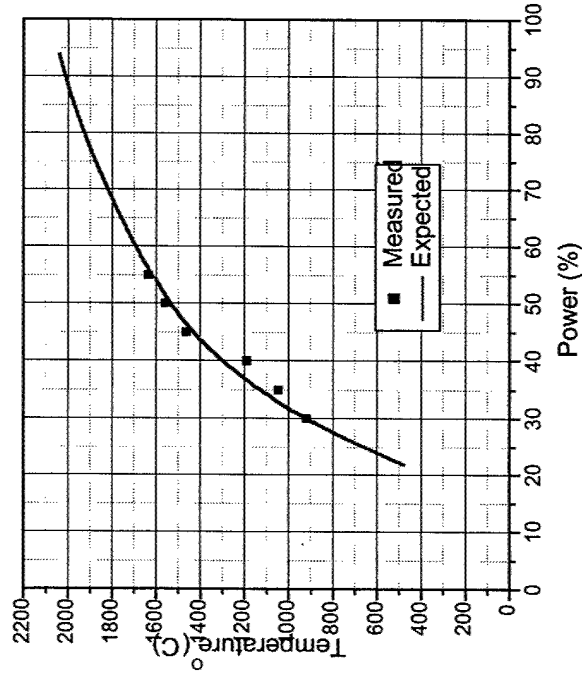


*Temperature measurement
Hot spot with Al₂O₃ tube
(OD : 5 mm, ID : 4 mm)*

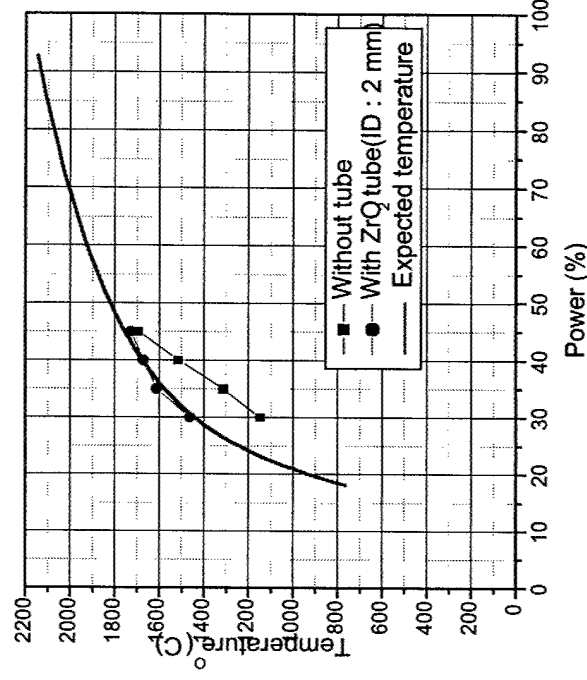


*Temperature measurement
with change of lamp and
tubes*

Temperature measurement

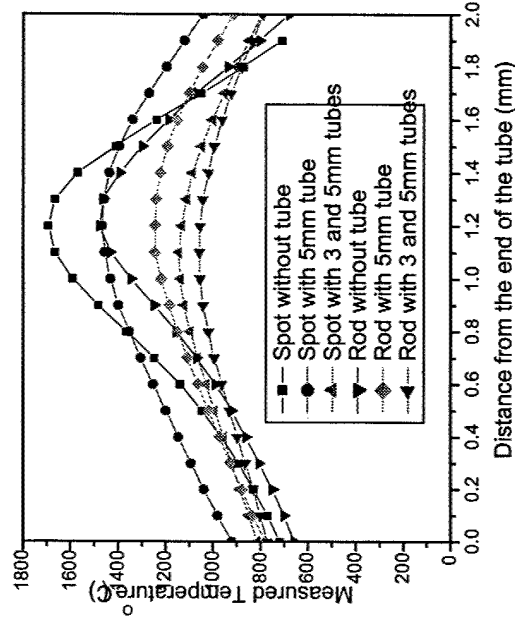
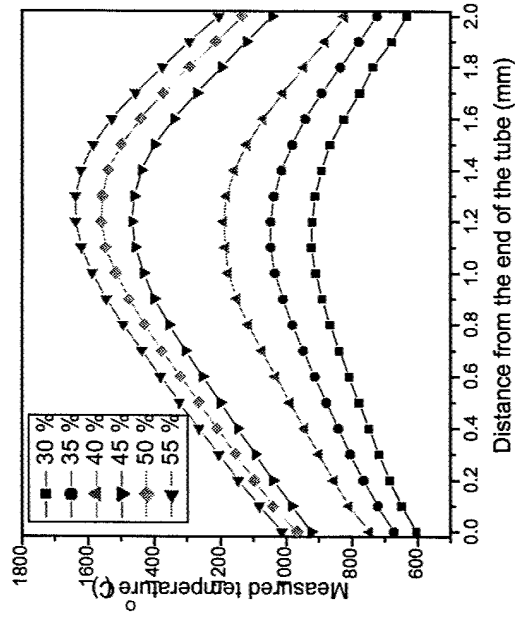


Measured vs. expected temperatures with one Al_2O_3 tube (OD : 5 mm, ID : 4 mm)



Measured vs. expected temperatures with one ZrO_2 tube (OD : 3 mm, ID : 2 mm)

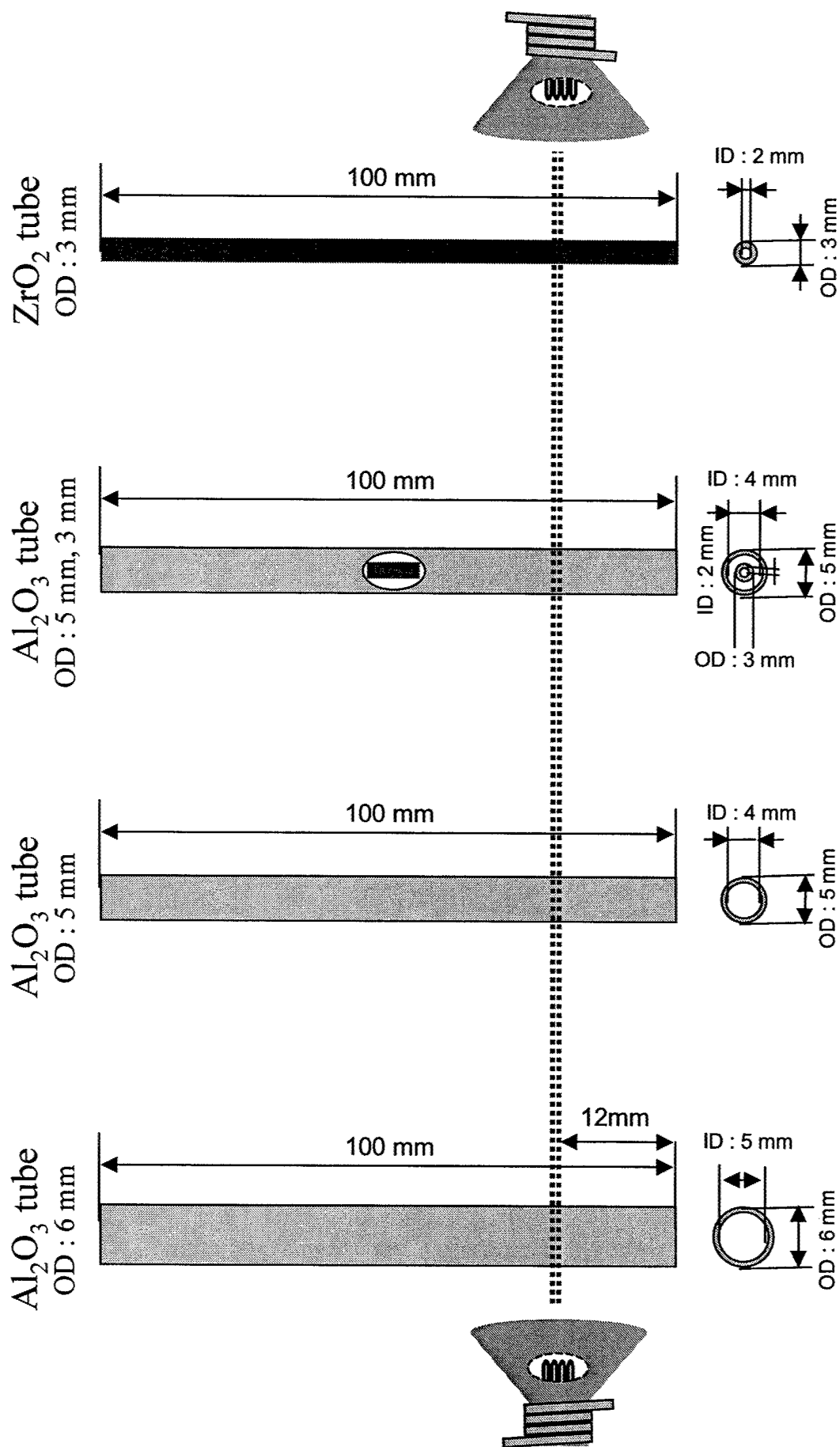
Temperature measurement



*Temperature measurement
Hot spot with 1 Al₂O₃ tube*

*Temperature measurement
with change of lamp and
tube configurations*

Tubes and lamp



Fibers

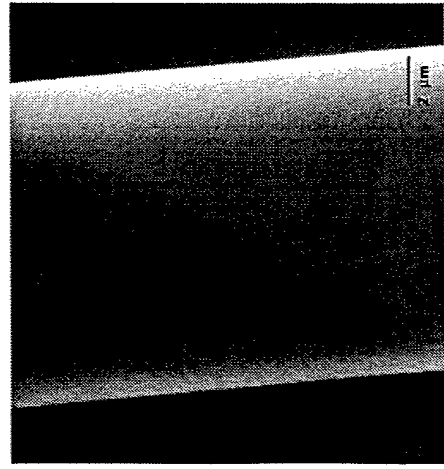
- Nextel fibers 550, 720
- Extruded mullite fibers
- Extruded YAG fibers

Nextel mullite based fibers

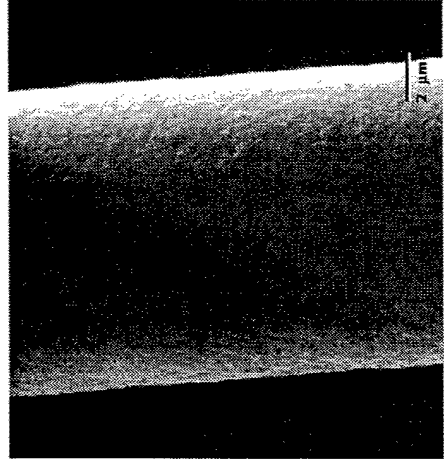
Property	Units	Nextel 312	Nextel 440	Nextel 550	Nextel 720
Sizing color	Color	White	coral	Blue	green
Chemical composition	wt. %	62.5 Al ₂ O ₃ 24.5 SiO ₂ 13 B ₂ O ₃	70 Al ₂ O ₃ 28 SiO ₂ 2 B ₂ O ₃	73 Al ₂ O ₃ 27 SiO ₂	85 Al ₂ O ₃ 15 SiO ₂
Melting point	°C	1800	1800	1800	1800
Filament diameter	µm	10-12	10-12	10-12	10-12
Crystal size	Nm	<500	<500	<500	<500
Crystal phase		Mullite + amorphous	<ul style="list-style-type: none"> -Al₂O₃ + Mullite + amorphous SiO₂ 	<ul style="list-style-type: none"> -Al₂O₃ + amorphous SiO₂ 	<ul style="list-style-type: none"> -Al₂O₃ + Mullite
Density	g/cc	2.70	3.05	3.03	3.40
Refractive index		1.568	1.614	1.602	1.67
Surface area	m ² /g	< 0.2	< 0.2	< 0.2	< 0.2
Filament tensile strength (25.4 mm gauge)	MPa ksi	1700 250	2000 290	2000 300	2100 300
Filament tensile modulus	GPa msi	150 22	190 27	193 28	260 36

SEM of Nextel 720 fibers

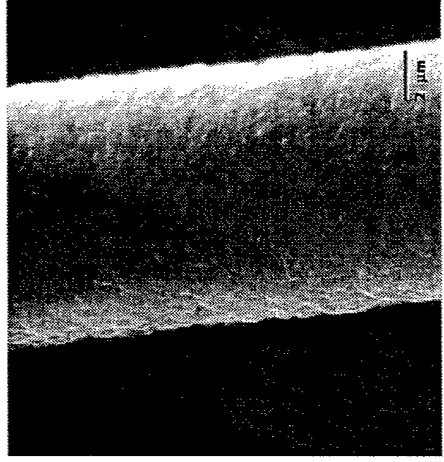
Heat treated in "hot rod" configuration with one alumina tube (OD: 6 mm)



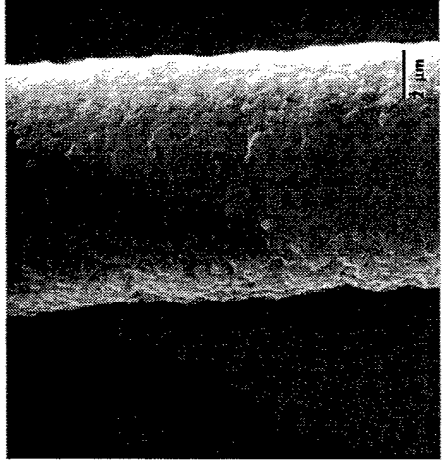
As-received



50%, 0.01mm/s

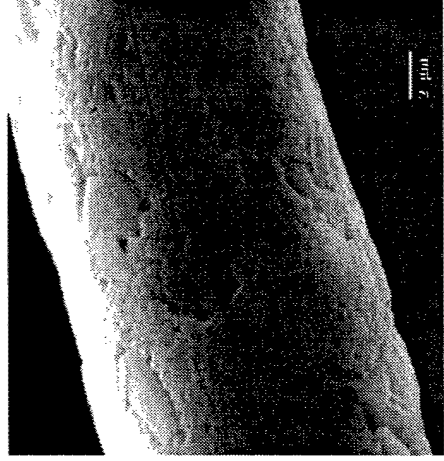
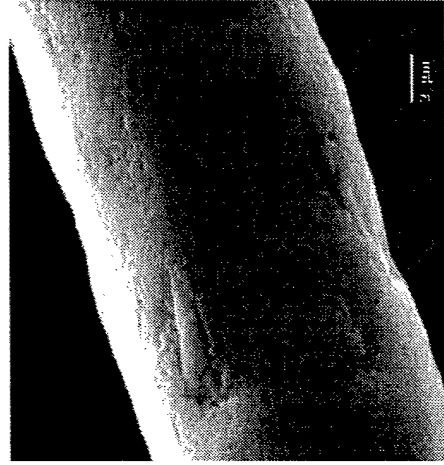


55%, 0.01mm/s



60%, 0.01mm/s

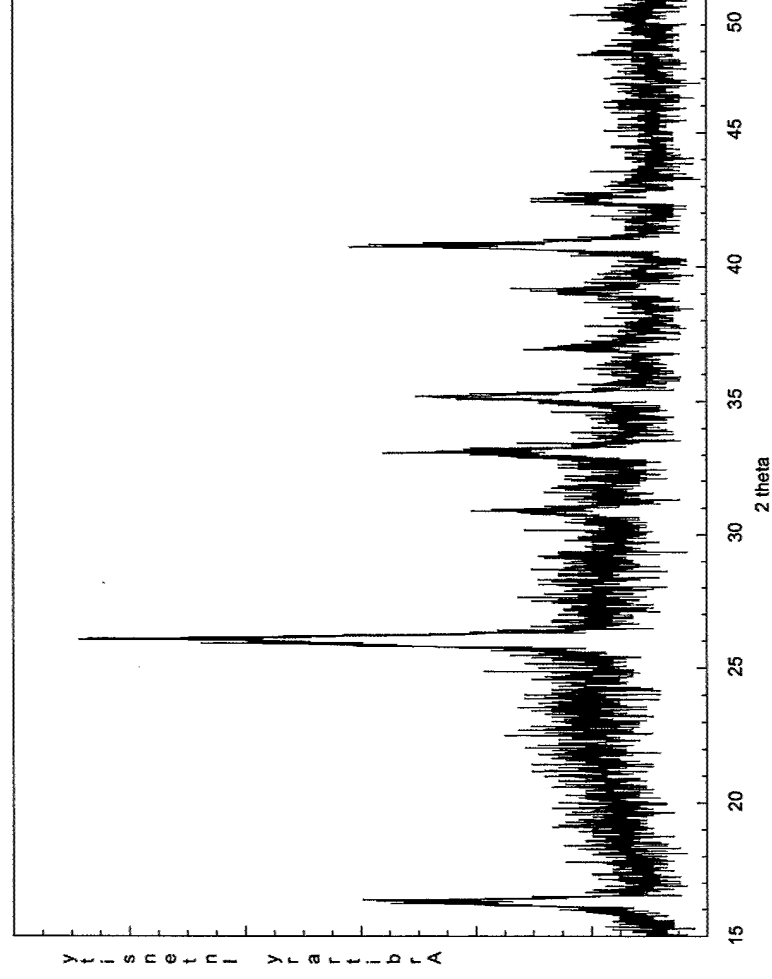
Power increase



Alumina phase

75%, 0.01mm/s
Heat treatment

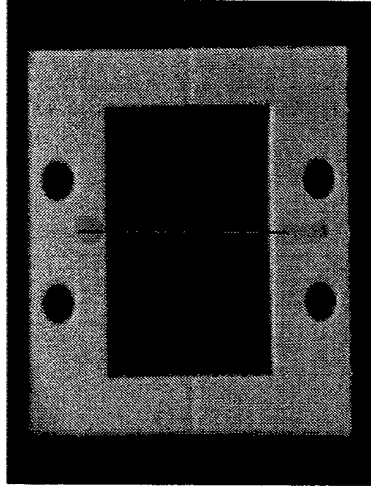
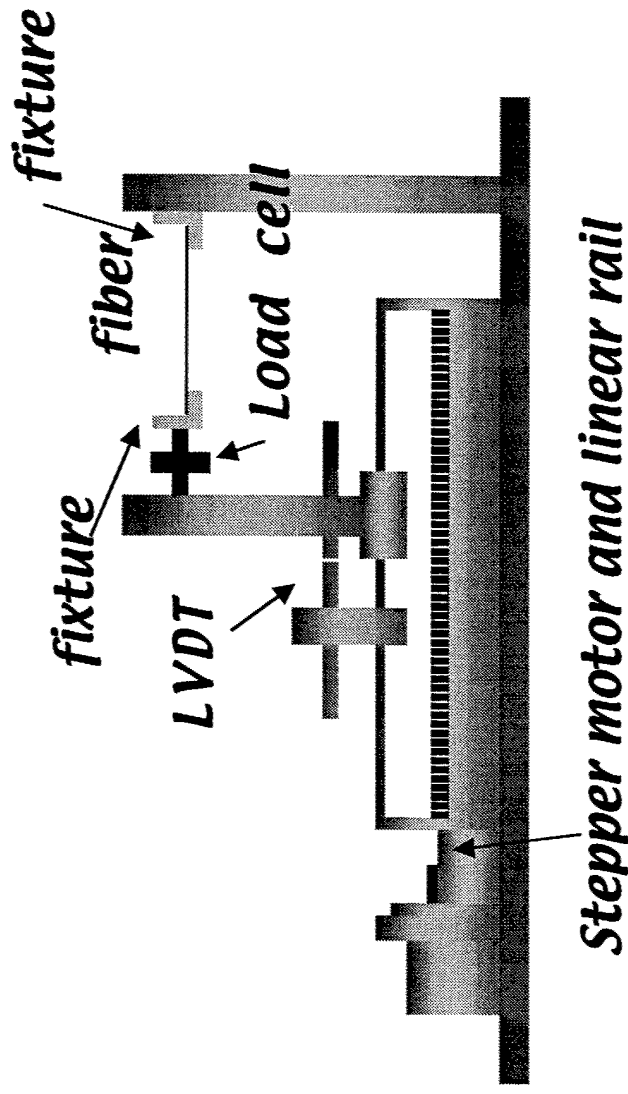
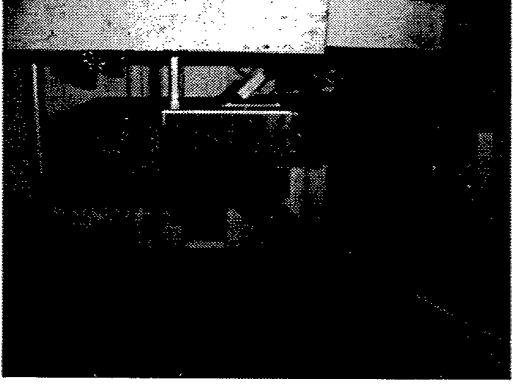
XRD of Nextel 550 Fibers



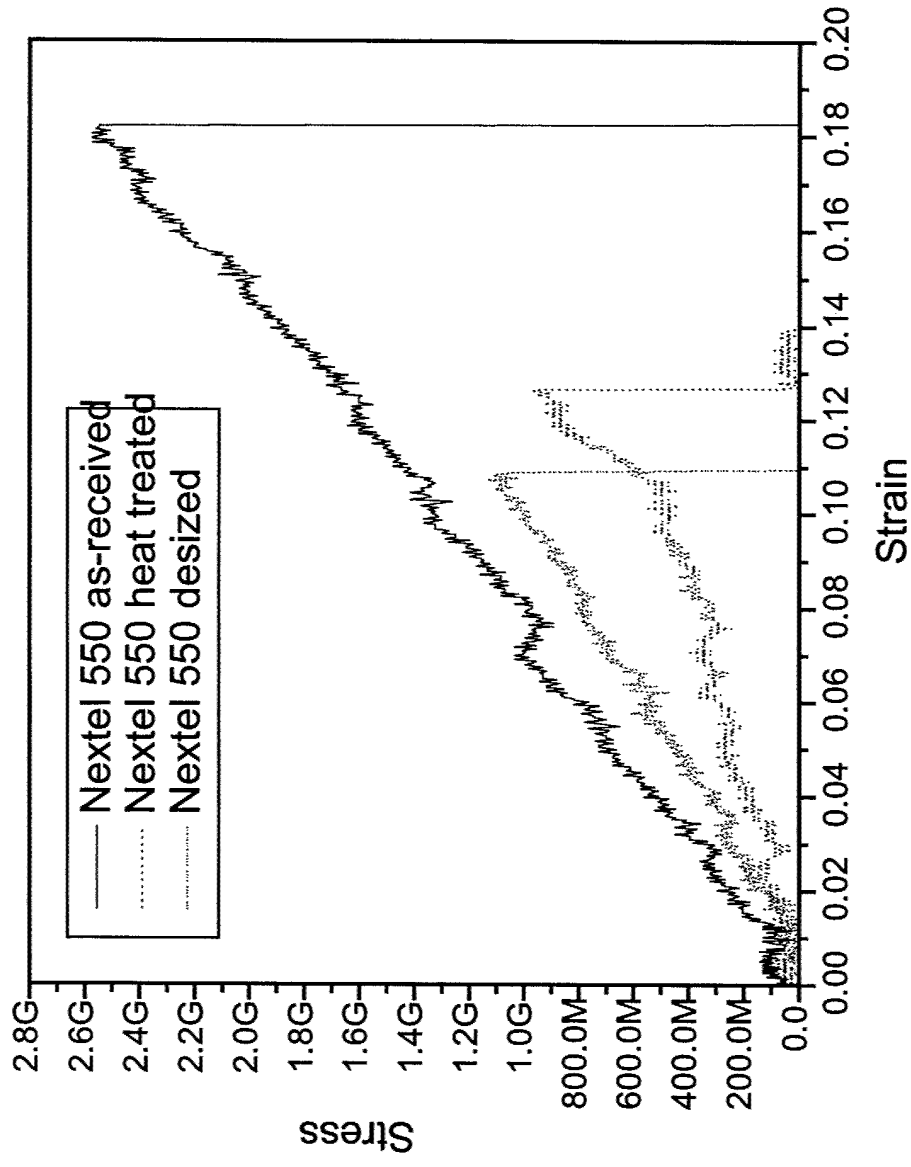
Mullite phase was synthesized after 60% of heat treatment in hot rod

Tensile test

- Tensile test can be done with Micropull™ (to 1400°C)
- ASTM D 3379-75
- 1"(25.4 mm) fiber or filament
- Creep test and high temperature strength can be measured



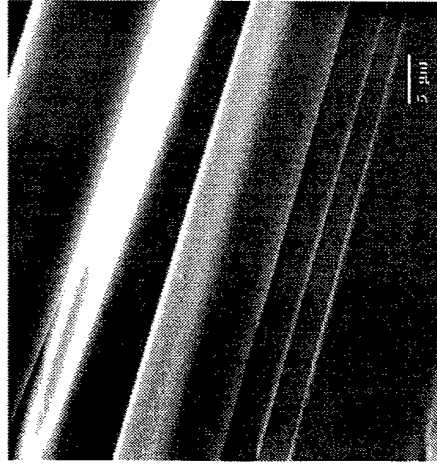
Tensile test of Nextel 550 fiber



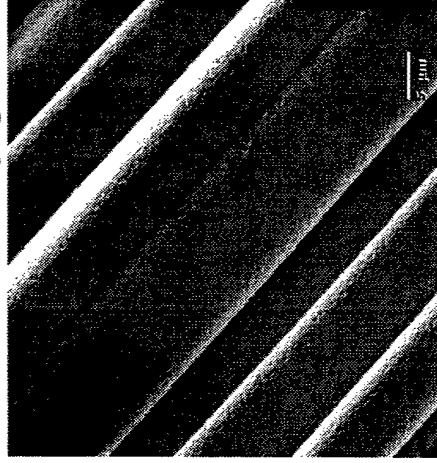
Tensile stress decreased with grain growth

SEM of Nextel 550 fiber tows

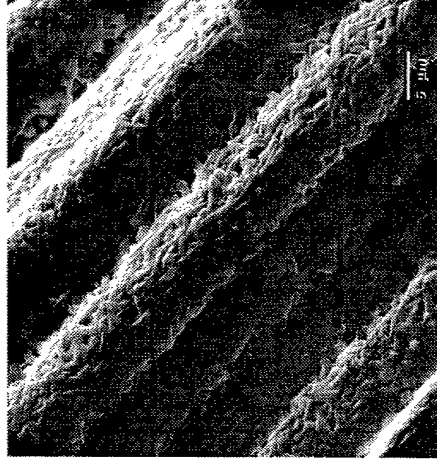
Heat treated in "hot rod" configuration with one alumina tube (OD: 6 mm)



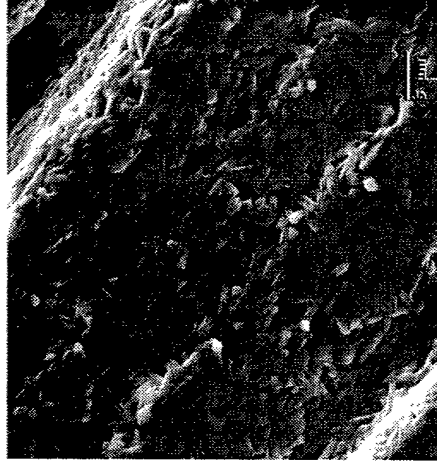
As-received



65%, 0.01mm/s

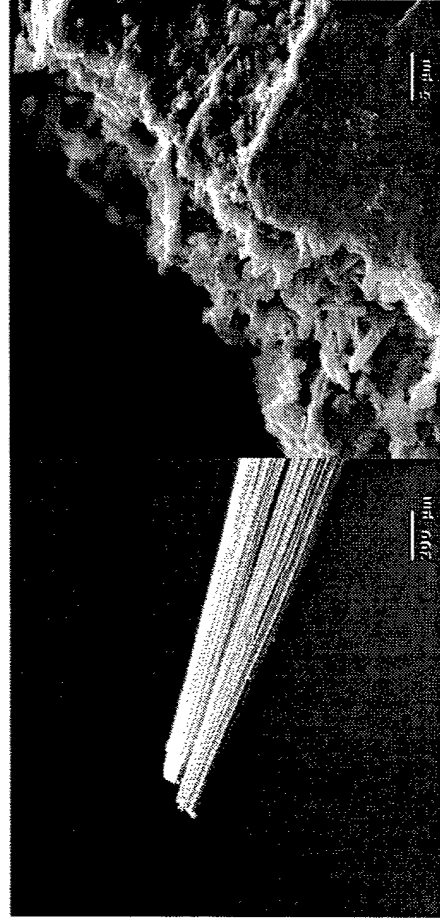


70%, 0.01mm/s



75%, 0.01mm/s

Power increase

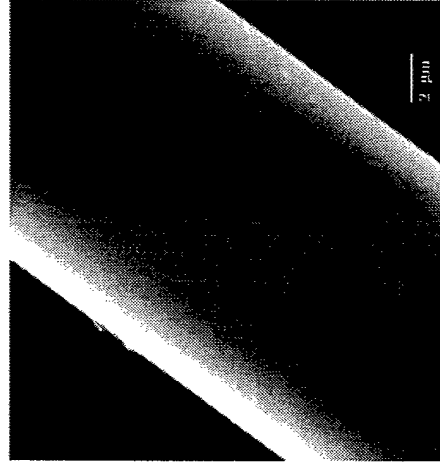


Broken part at 85%, 0.01mm/s

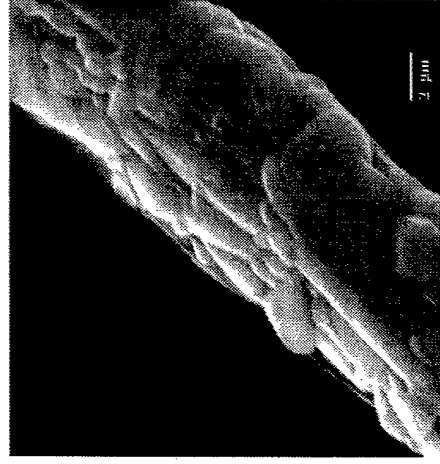


Single filament heat treated with load at 60%, 0.01mm/s

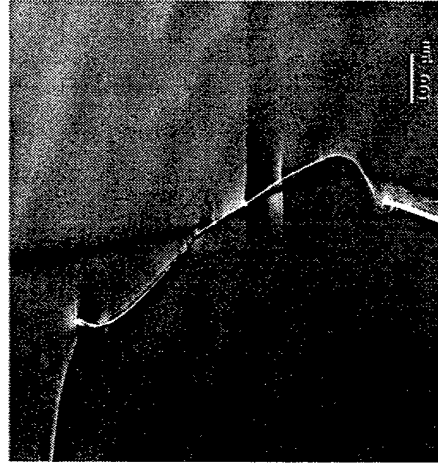
SEM of Nextel 550 fiber



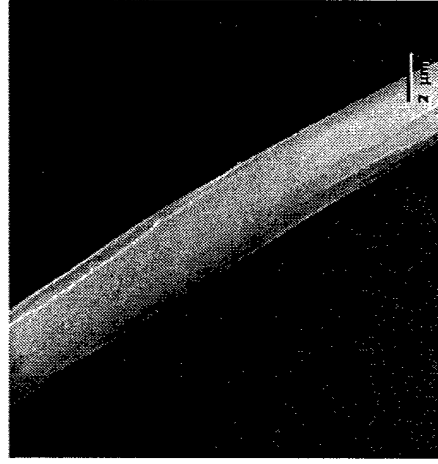
As-received



Grain growth in the fiber
at 75%, 0.01 mm/s heat treatment
hot rod with one alumina tube (OD: 6 mm)

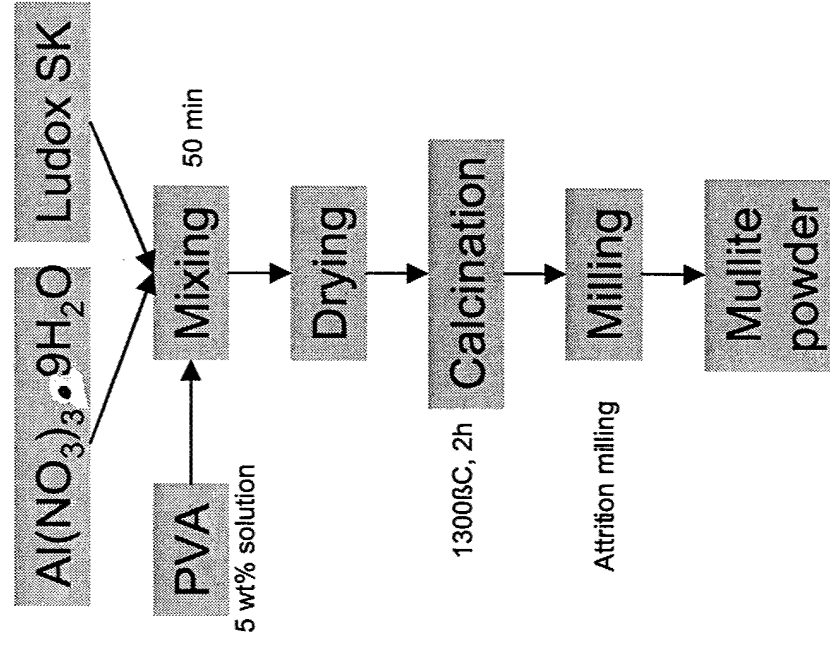


Micro mullite fiber grown by pedestal
method at 80%, 0.05 mm/s
hot rod with one alumina tube (OD: 6 mm)

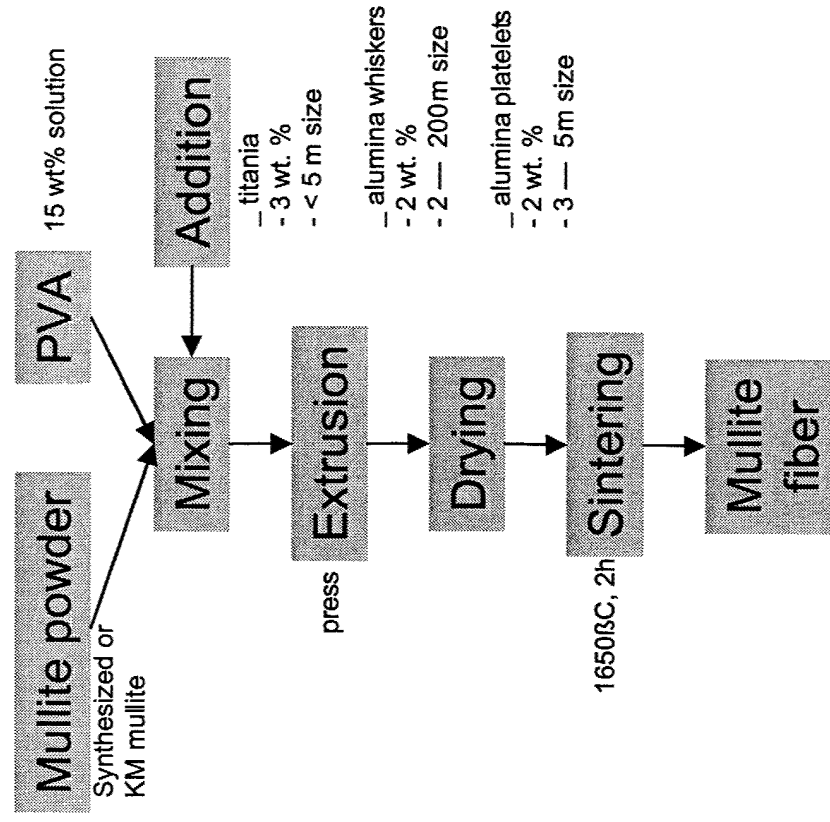


Mullite Fibers

Mullite powder synthesis

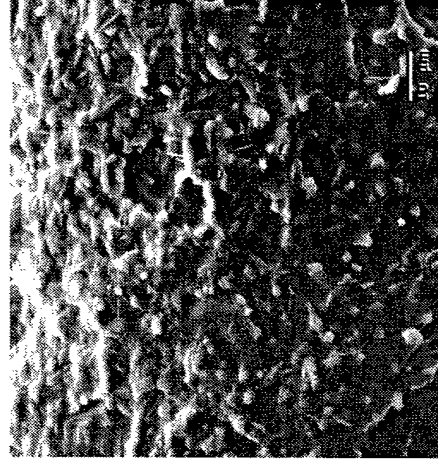
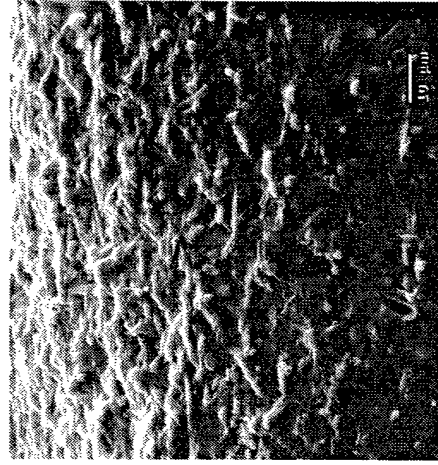
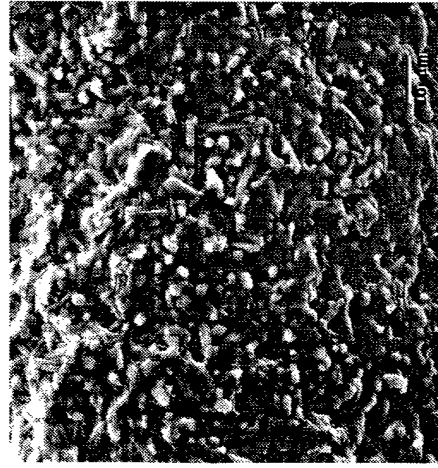


Mullite fiber making



SEM of mullite fibers

*Heat treated in "hot rod" configuration with one alumina tube (OD: 6 mm)
as function of position along tube towards as "hot rod"*



Power increase

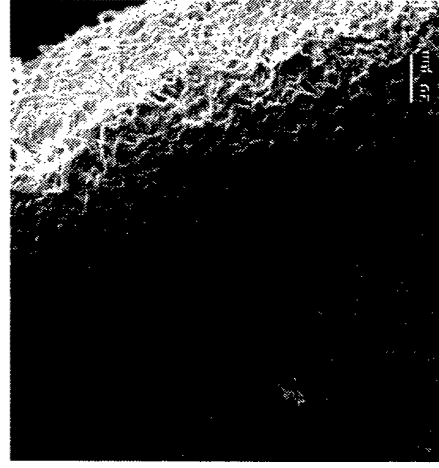


Alumina

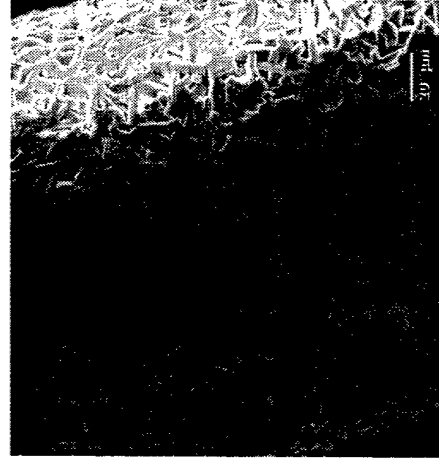
75%, 0.01mm/s
Heat treatment

SEM of mullite fibers

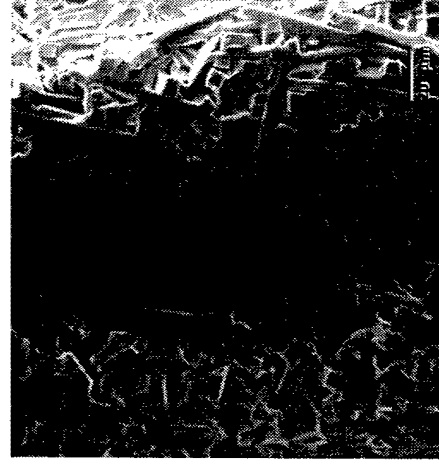
Heat treated in "hot rod" configuration with one alumina tube (OD: 6 mm)



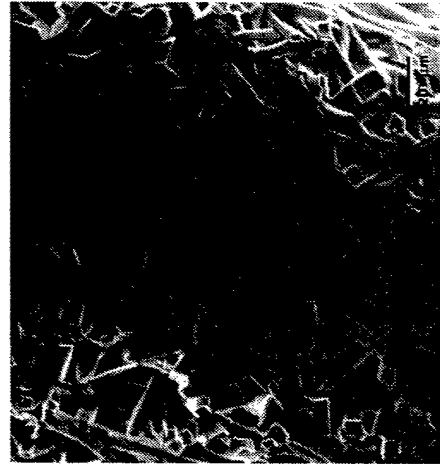
After pre-sintering at 1650°C/2h



65%, 0.01mm/s



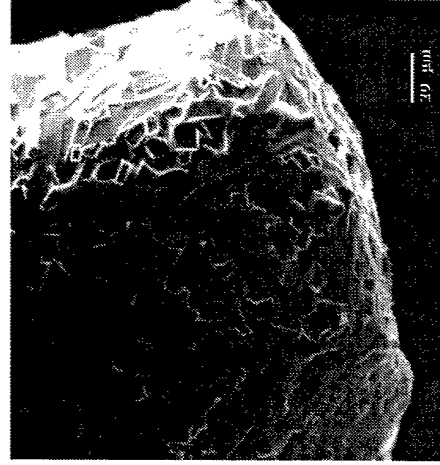
75%, 0.01mm/s



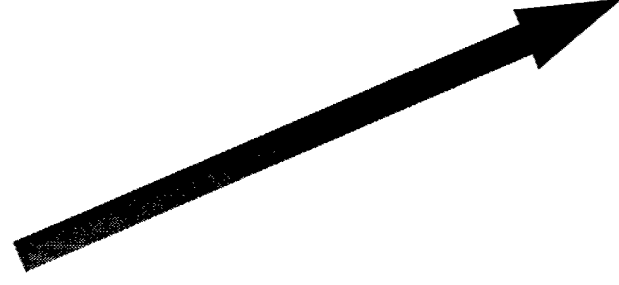
80%, 0.01mm/s



85%, 0.01mm/s



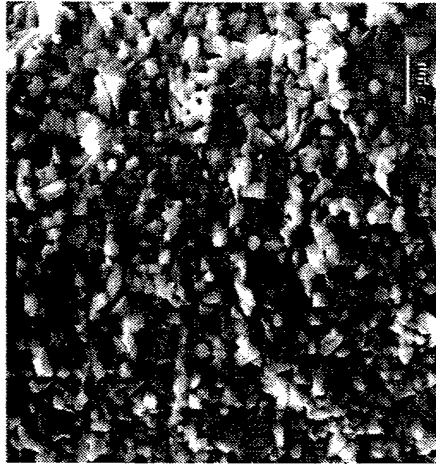
85%, 0.01mm/s



Power increase

SEM of titania added mullite fibers

Heat treated in "hot spot" configuration with one alumina tube (OD: 5 mm)



After pre-sintering at 1650°C/2h



60%, 0.01mm/s



62%, 0.01mm/s



65%, 0.01mm/s

Power increase



Alumina whiskers
added

75%, 0.01mm/s
Heat treatment

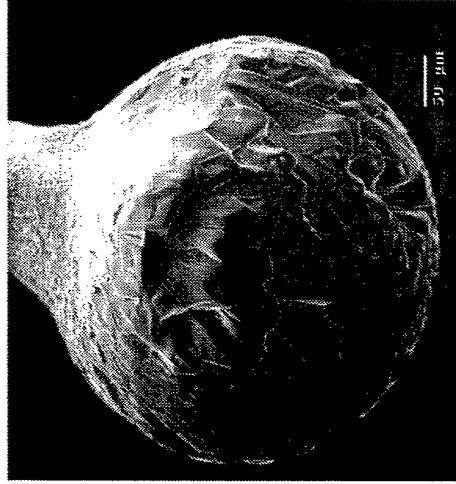


Alumina platelets
added

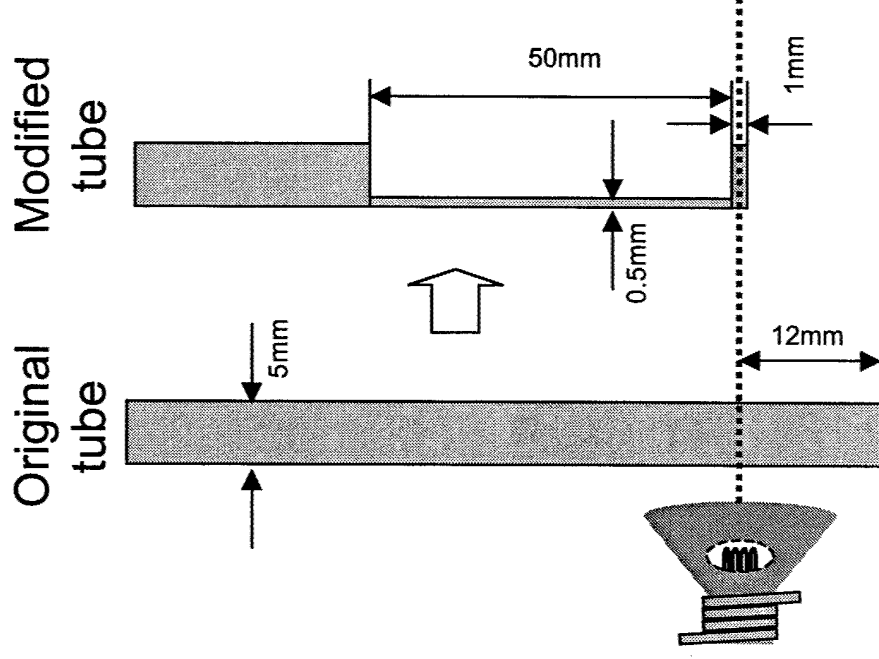
75%, 0.01mm/s
Heat treatment

SEM of mullite fibers

*Heat treated in "hot spot" configuration with one modified alumina tube
KM mullite with titania addition*

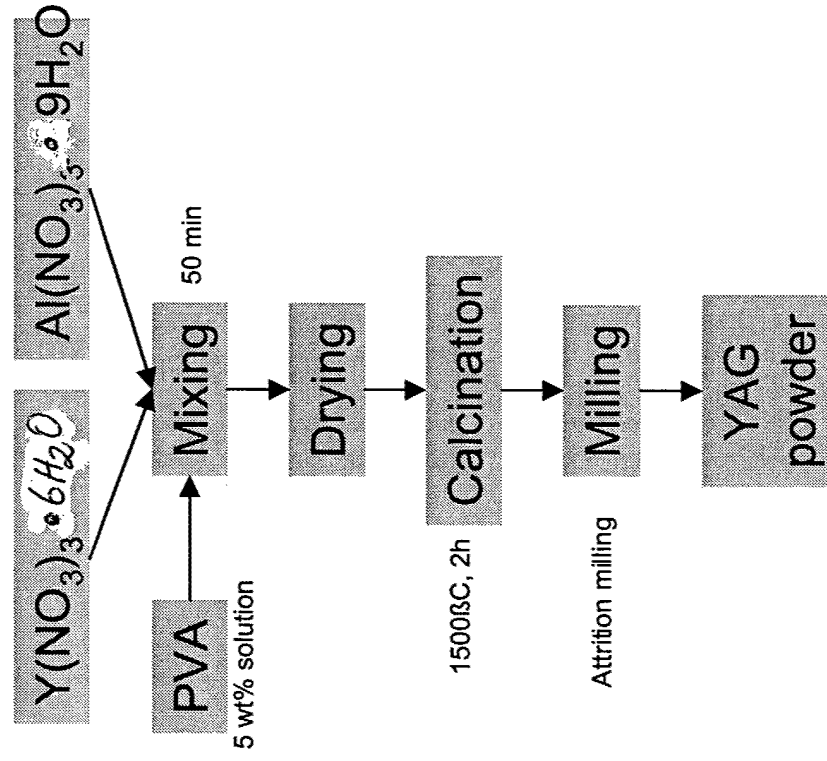


82%, 0.01mm/s
Heat treatment

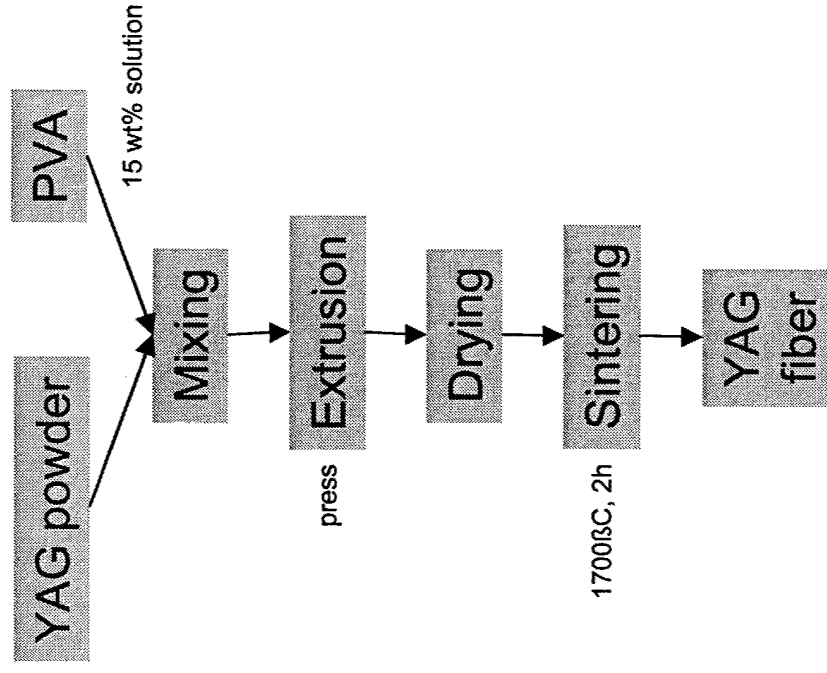


YAG Fibers

YAG powder synthesis

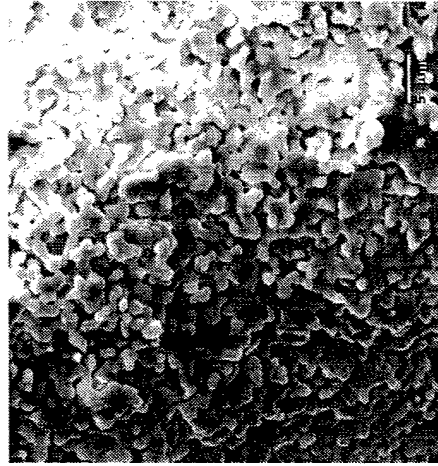


YAG fiber making

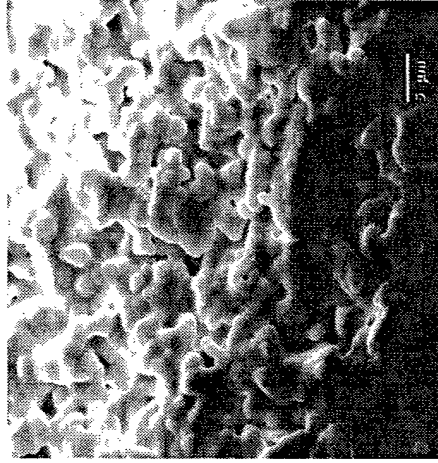


SEM of YAG fibers

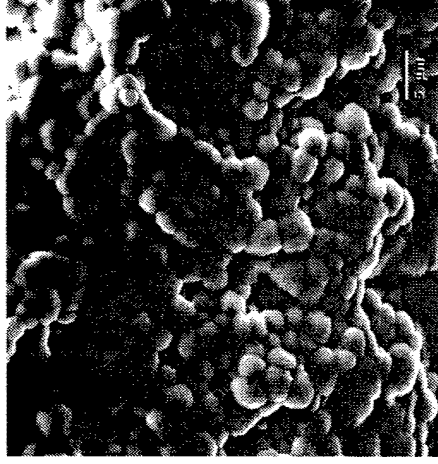
Heat treated in "hot spot" configuration with one alumina tube (OD: 5 mm)



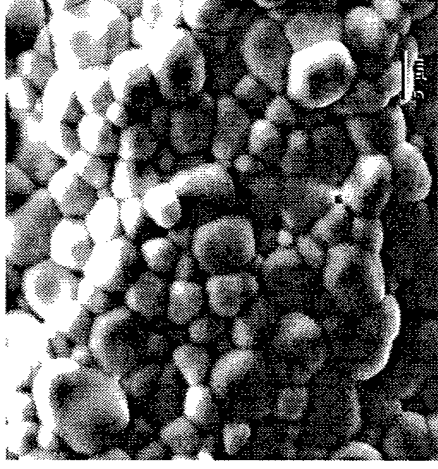
After pre-sintering at 1700°C/2h



60%, 0.01mm/s

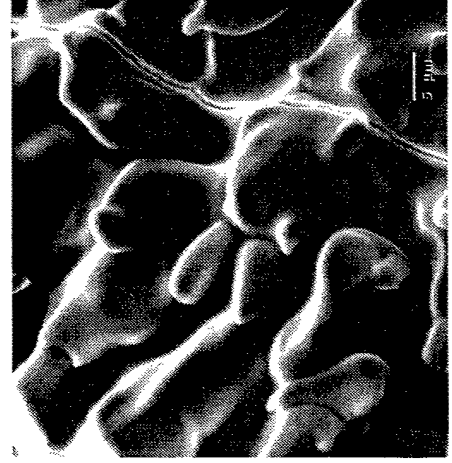


70%, 0.01mm/s



80%, 0.01mm/s

Power increase



Molten region of
YAG fiber

90%, 0.01mm/s (16cm/min)

Heat treatment

With zirconia tube

OD : 3mm, ID 2mm

Conclusions

- We have built and calibrated a four-lamp, image furnace, having a narrow hot zone and capable of operating to 2000°C in air
- Heat treatments can be controlled by two parameters of temperature and traverse rate (from 0.1 $\mu\text{m}/\text{sec}$ to 0.025 m/sec, or 1 inch/sec)
- Grain growth, densification and melting can be achieved in monofilaments, indicating the feasibility of making textured or single crystal fibers in a continuous process.
- We have developed a process to extrude polycrystalline powders of green diameters $\Phi \sim 140 \mu\text{m}$, which densify to $\Phi \sim 100 \mu\text{m}$ or less
- Nextel 550, 720, pure and Ti O₂-doped mullite fibers have been heat treated or melted, and a textured microstructure has been achieved